Hindawi
Advances in Materials Science and Engineering
Volume 2023, Article ID 7995789, 7 pages
https://doi.org/10.1155/2023/7995789

*Research Article*

# Microstructure Evolution and Work Hardening Behavior of Hot-Rolled DP780 Ferrite/Bainite Dual-Phase Steel

**Zhengtuan Li,[1,2] Chunjing Wu,[1] and Heli Wan [2]**

[1]*School of Materials Science and Engineering, University of Science and Technology Beijing, Beijing 100083, China*
[2]*HBIS Chengde Iron and Steel Group Co., Ltd., Chengde 067000, China*

Correspondence should be addressed to Heli Wan; wanheli@163.com

Received 6 July 2022; Revised 2 November 2022; Accepted 27 January 2023; Published 7 April 2023

Academic Editor: Baskaran Rangasamy



In this article, by optimizing the alloy composition, the DP780 grade hot-rolled duplex steel was obtained by TMCP (thermo-mechanical control process) combined with medium temperature coiling procedure. The microstructure evolution and mechanical properties of the experimental steel were analyzed by means of optical microscopy (OM), scanning electron microscopy (SEM), transmission electron microscopy (TEM), room temperature tensile experiment, and low-temperature impact experiment. When the coiling temperature was 540°C, the yield strength, tensile strength, and elongation of the experimental steel were 663 MPa, 785 MPa, and 23%, respectively, and the product of the strength and elongation was as high as 18.1 GPa%, which accords with the mechanical properties of the national standard for DP780 dual-phase steel. The experimental steel exhibits significant work hardening effect at higher strain, and can still guarantee a certain work hardening index and good formability. When the coiling temperature was high (570°C), the strength of the experimental steel decreased and the work hardening effect was also weakened due to the coarsening of microstructure. The results of this article provide theoretical guidance for the production of DP780 dual-phase steel by hot rolling.

## 1. Introduction

With the development of TMCP (thermo-mechanical control process) technology, hot rolling process can be used to produce thin strip produced by cold rolling process, and the production range can be broadened, shortened production cycle, and energy saving, and emission reduction can be achieved by "replacing cold rolling with hot rolling" [1, 2]. Replacing cold rolling with hot rolling has gradually become the development direction of major steel mills to improve production efficiency and reduce production costs [3, 4]. Hot-rolleddual-phase steel has the characteristics of high strength, low yield ratio, continuous yield and high initial hardening rate, which can meet the combination of high strength and cold forming, excellent welding performance and fatigue performance [5], and it is considered an ideal steel for automobiles [6]. Compared with traditional ferritic/martensitic dual-phase steel, ferrite/bainite dual-phase steel (FB steel) has good strength and toughness matching and extended flange performance [7, 8] and is widely used by the moving parts such as car chassis and spokes.

At present, NKK of Japan, POSCO of South Korea, ThyssenKrupp of Germany, and SSAB of Sweden are in the forefront of FB steel research in the world and have successfully developed DP600, DP780, and higher-gradehot-rolleddual-phase steels [9, 10]. Besides, Gao et al. developed a the strength-ductility synergy of dual-phase (DP) steels that was obtained by properly tailoring the structural heterogeneity, including the distribution and fraction of constituent phases [11–14]. Due to the lower yield strength, good performance stability, and uniformity of DP780 steel, it has broad market application prospects. Therefore, different experimental conditions were studied in this article.

Hot-rolleddual-phase steels for automobiles produced by domestic steel mills are mainly below 600 MPa [15], and higher-strengthdual-phase steels require cold rolling combined with annealing processes, which have a long

production cycle [16–19]. However, research on the production of high-strengthDP780-gradehot-rolleddual-phase steel through bainite transformation interval coiling is relatively lacking. In this article, by adopting V-N-Cr microalloying design, using TMCP process combined with medium temperature crimping process, DP780 grade ferrite/bainite dual-phase steel is obtained, and the microstructure evolution and mechanical properties are studied, and the work hardening behavior of the experimental steel is analyzed. The research results provide reference and basis for the process determination and production of hot-rolled DP780 grade dual-phase steel.

## 2. Experimental Details

The chemical composition of the experimental steel is shown in Table 1, and the balance is Fe. The phase diagram of the experimental steel was calculated by Thermo-Calc. The specific results are shown in Figure 1. The measured $A_1 = 678^{\circ}C$, $A_3 = 830^{\circ}C$ the cementite precipitation temperature is around 685°C, and the V (C, N) is in the equilibrium state. The precipitation begins at 1100°C and reaches the maximum at 700°C. A vacuum melting furnace was used to smelt the experimental steel into ingots, then the ingots were forged into long billets, and hot-rolled experimental billets of appropriate length were cut for rolling experiments. The specific controlled rolling and controlled cooling process is shown in Figure 2. A billet of $80 \times 90 \times 110$ mm is heated in a box-type heating furnace to 1200°C and held for 2 hours. When it is air-cooled to 1100°C, the first stage of austenite recrystallization zone rolling is carried out. The billet is from 80 mm. After 2 passes, it is thinned to 45 mm (rough rolling), and then air-cooled to 900°C in the second stage of rolling in the austenite unrecrystallized zone. The steel plate is finally rolled into 10 mm thick strip after 5 passes (Finish rolling), the pass reduction is controlled between 20% and 25%, and the final rolling temperature is controlled around 850°C. The strip is cooled to 570°C and 540°C by water quenching (30–40°C/s), and then is coiled by a coiler and slowly cooled to room temperature. For ease of description, the experimental steel coiled at 570°C is recorded as steel A, and the experimental steel coiled at 540°C is recorded as steel B.

Metallographic specimens were cut from the side of the rolled plate along the rolling direction. After grinding and mechanical polishing, they were corroded by 4% nitric acid alcohol solution (volume percentage). The microstructures of different coiling temperatures were taken by OLYMPUS optical microscope (OM) and Zeiss Ultra 55 Field emission scanning electron microscope (SEM) was used for observation, and the fine structure and precipitates of the sample were observed by FEI Tecnai G2 F20 transmission electron microscope (TEM). Electron backscatter technology (EBSD) was used to analyze the phase distribution and grain boundary angle distribution in the microstructure. The sample was prepared by electrolytic polishing with a 12.5% vol perchlorate alcohol solution (volume percentage), and then measured on a Zeiss Ultra 55 field emission scanning electron microscope with 0.06 $\mu$m Step size scans point by point.

Table 1: Chemical composition of experimental steel (wt%).

| | |
|---|---|
| C | 0.08 |
| Si | 0.27 |
| Mn | 1.80 |
| Cr + Mo | 0.71 |
| V | 0.103 |
| N | 0.0155 |
| P | 0.015 |
| S | 0.002 |

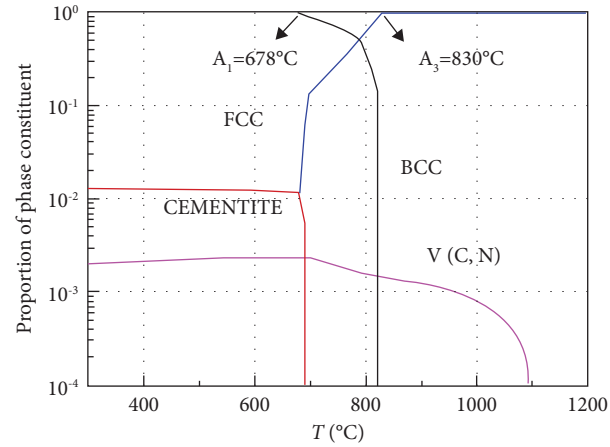


Figure 1: Phase diagram calculation for experimental steel based on thermo-calc.

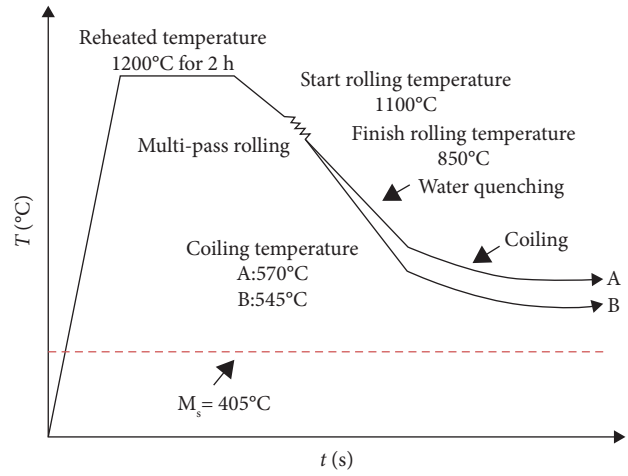


Figure 2: Schematic diagram of hot rolling and cooling process.

According to GB/T 2975 national standard, take the full-thickness standard tensile plate sample along the rolling direction. At room temperature, assume that the strain rate is 3 mm/min on the CMT5105 microcomputer controlled universal testing machine according to GB/T 228-2002 "Metal Tensile Test Method" to conduct a tensile test. Charpy V-type impact test is taken along the width and extension direction. The size of the sample is $5 \times 10 \times 55$ mm (1/2 standard sample). It is carried out on the MTS ZBC2452-B pendulum test machine according to ASTME 23, and the test temperature is −20°C, after the impact test is

completed, observe the fracture morphology of the sample on the FEI QUANTA 600 scanning electron microscope. Each experimental result is determined by more than three experimental data, so as to ensure the accuracy of the experimental results.

## 3. Results and Discussion

*3.1. The Influence of Coiling Temperature on Microstructure.* The optical microstructure and secondary electron image of the experimental steel are shown in Figure 3. It can be observed from Figure 3(a) that when the coiling temperature is 570°C, the microstructure in steel A is a typical granular bainite structure, which is a mixture of ferrite and islands surrounded by it. The structure, in which the black spheres are retained austenite or M-A structure, under the electron microscope, it appears as a convex block structure, as shown in Figure 3(b). When the coiling temperature is 540°C, the microstructure of steel B contains granular bainite and a small amount of acicular ferrite, and the M-A structure is relatively small, as shown in Figure 3(d). The ferrite volume fraction of steel A is 63.3%, which is shown in Figure 3(b), and the ferrite volume fraction of steel B is 64.1% as shown in Figure 3(d). There is little difference in the amount of ferrite introduced between the two, which is mainly related to the rolling process and is the same as the cooling process before coiling. For the steel in this experiment, the microstructures obtained at these two coiling temperatures are ferrite + bainite type dual-phase steels. As a soft phase structure, ferrite can ensure the plasticity of the steel to a certain extent, and at the same time, it still has good ductility. The rate is better than the full bainite structure, and bainite as a hard phase structure ensures the strength of the steel.

The crystallographic characteristics of the experimental steel were analyzed by EBSD technology, and the experimental results are shown in Figure 4. Figures 4(a) and 4(d) are the quality maps of steel A and steel B, respectively. The colored massive structure is retained austenite, which is distributed near the ferrite grain boundary, and different colors represent different orientations. The retained austenite in steel A is small, while the size of retained austenite in steel B is different. This may contribute to the plasticity of the experimental steel, because the retained austenite is prone to normal strain and reduces the stress concentration at the crack tip. It causes crack propagation, dullness, and other normal deformation, which is manifested by phase change induced plasticity (TRIP) [16]. It can be found that black massive structures are found in the quality maps of steel A and steel B, which are high-carbon martensite. The high-carbon martensite lattice distortion is large and the band contrast value is low, so the color in the quality map is darker. Figures 4(b) and 4(e) are the orientation maps of steel A and steel B, respectively. The color shades at different positions represent different orientation relationships, and the orientation difference of steel B is relatively large. Figures 4(c) and 4(f) are the grain boundary distribution maps of steel A and steel B, respectively, and the corresponding azimuth angle and grain boundary ratio relationship diagrams are shown in Figures 4(g) and 4(h). Generally speaking, those with an orientation angle between 2° and 15° are small-angle grain boundaries, and those with an orientation angle above 15° are high-angle grain boundaries. The large-angle grain boundary can hinder the movement of dislocations during the deformation process, which helps to improve the strength of the steel [13], and a large proportion of the large-angle grain boundary determines the crack propagation work and can improve the impact toughness [17]. By comparison, the ratio of high-angle grain boundaries of steel B is 62.2%, which is higher than that of steel A (49.3%).

In order to analyze the fine structure of the experimental steel more accurately, the morphology of the structure was observed under a transmission electron microscope. The specific morphology is shown in Figure 5. Figure 5(a) shows the TEM morphology of steel A. The granular bainite is a fine lath structure under TEM, which is different from the spherical morphology under OM, and there is a twin martensite structure in steel A. The formation of twinned martensite is mainly due to deformation and carbon desorption of ferrite. Some austenite with high-carbon content but unstable morphology undergoes martensite transformation during the quenching process, and its substructure is twinned [17]. Large-sized square and spherical precipitates were found on the ferrite matrix, as shown in Figure 5(b). The element distribution of the precipitates at the dotted line in the figure is shown in Figure 5(c). The precipitates are VC (vanadium carbide). In steel B, finer spherical VC precipitates with a size of about 40 nm were found, as shown in Figure 5(d), and the corresponding energy spectrum is shown in Figure 5(f). It can be observed that there are fine and dispersed nano-scale precipitates on the ferrite matrix, and there are more entangled dislocations on the hard phase structure adjacent to the ferrite, as shown in Figure 5(e). Dislocation strengthening and precipitation strengthening are important strengthening methods for this experimental steel. More important, it can be clearly seen from Figures 4(a) and 4(b) that the quantity of retained austenite in steel B is more than that in steel A, due to the reduction of coiling temperature is conducive to the transformation of martensite into austenite and retained austenite is also an important aspect to improve ductility. Therefore, ductility of steel B is significantly improved. As shown in Figure 6(a).

*3.2. The Influence of Coiling Temperature on Mechanical Properties.* Figure 6 is an analysis diagram of the mechanical properties and work hardening behavior of two experimental steels. Figure 6(a) is the engineering stress-engineering strain curve. It can be found that the dual-phase steel has the characteristic of continuous yielding, which is caused by the existence of internal stress, which allows the dislocation to remain mobile [18, 19]. The yield strength, tensile strength, and elongation of steel A with higher coiling temperature are 620 MPa, 764 MPa, and 17% respectively. When the coiling temperature is lowered, the yield strength, tensile strength, and elongation of steel B are 663 MPa, 785 MPa, and 23%. The strong plastic product of

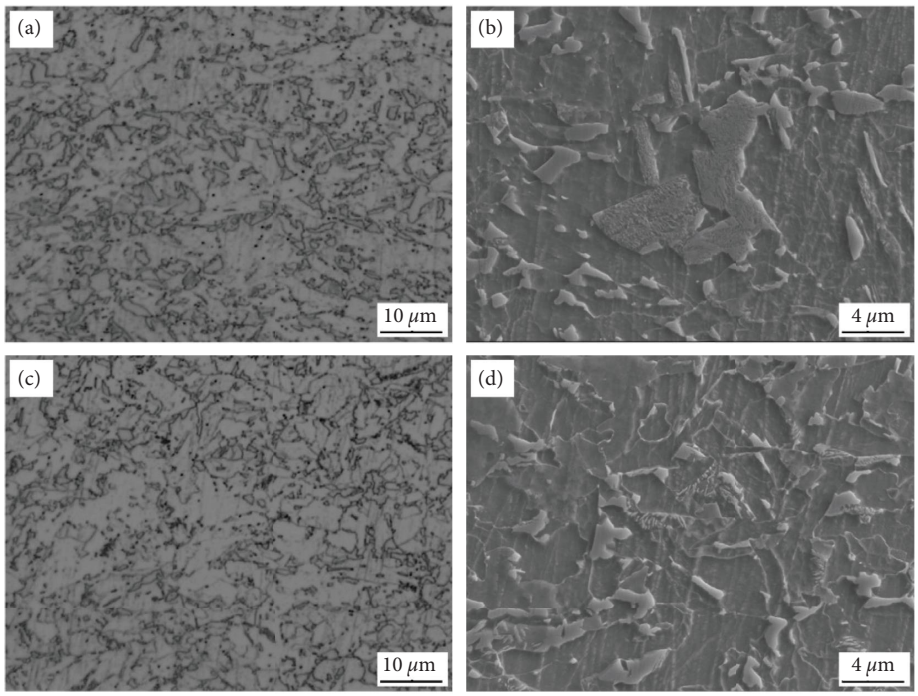


Figure 3: Microstructure images of experimental steels. (a, b) OM micrograph and SEM micrograph of steel A. (c, d) OM micrograph and SEM micrograph of steel B.

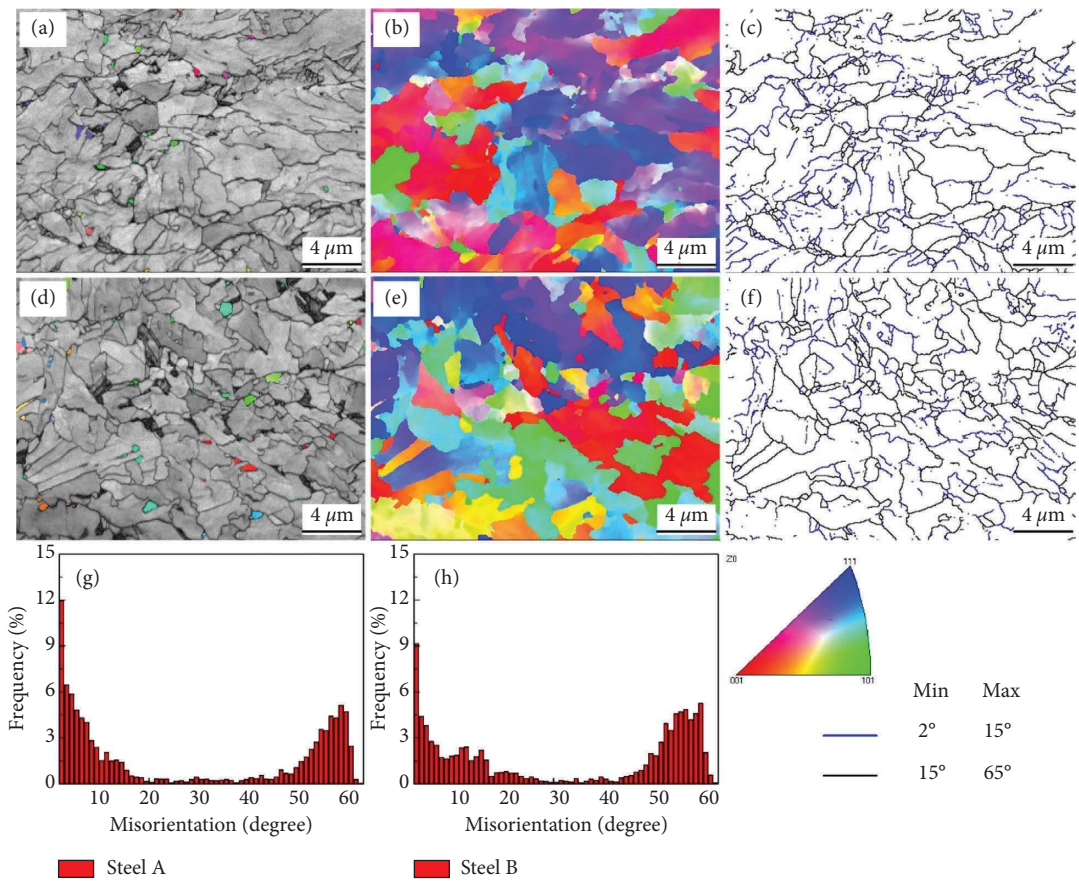


Figure 4: Crystallographic characteristics of experimental steels analyzed by EBSD: (a–c) image quality map, orientation image map, and grain boundary misorientation map of steel A; (d–f) image quality map, orientation image map, and grain boundary misorientation map of steel B; (g) plot of misorientation angle versus percentage of steel A; and (h) plot of misorientation angle versus percentage of steel B.

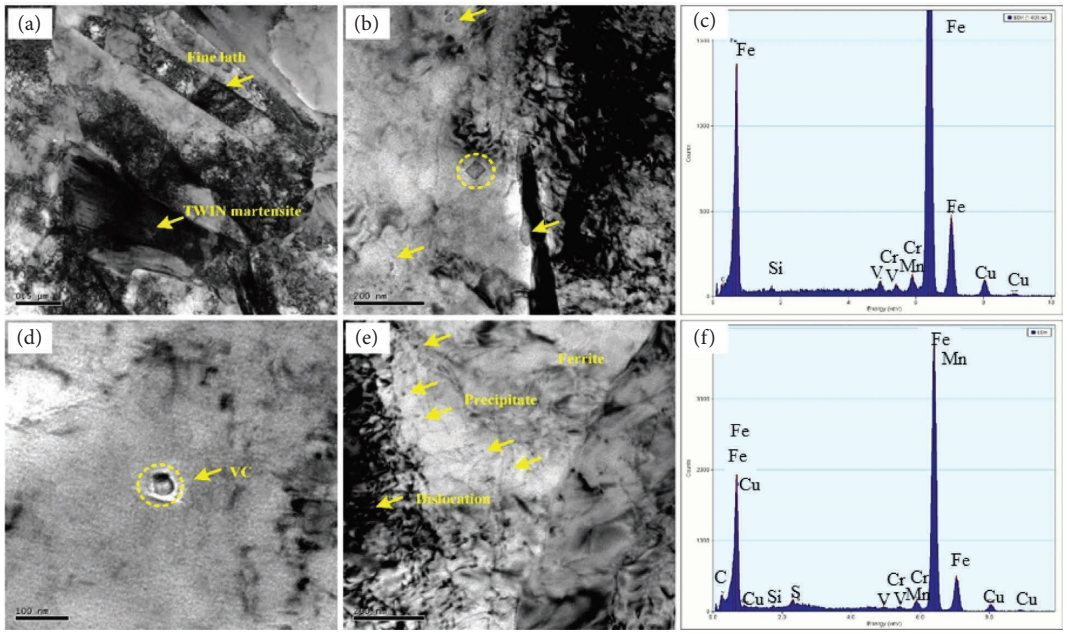


Figure 5: TEM micrographs of experimental steels: (a) morphology of granular bainite in steel A as coiling temperature is 570°C; (b) morphology of precipitates in steel A as coiling temperature is 570°C; (c) chemical composition of precipitates in steel A as coiling temperature is 570°C; (d) fine VC precipitate in steel A as coiling temperature is 570°C; (e) fine precipitates on ferrite in steel A as coiling temperature is 570°C; and (f) chemical composition of precipitates in steel B as coiling temperature is 540°C.

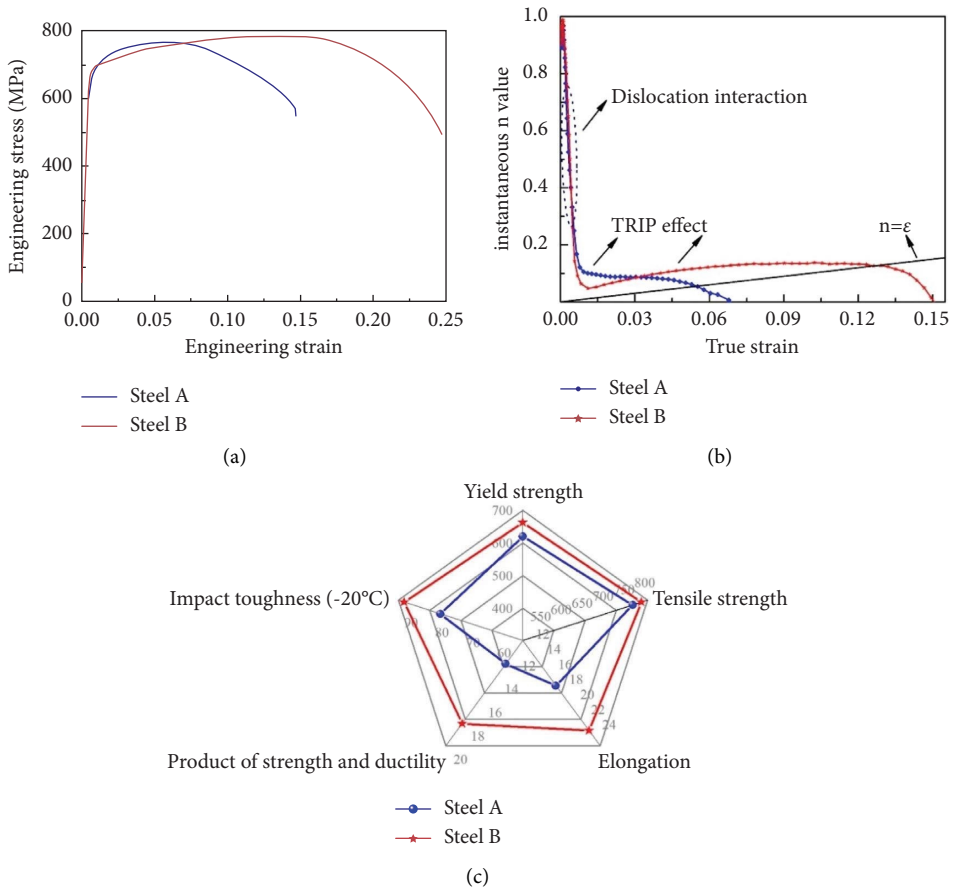


Figure 6: Mechanical properties and work hardening behavior: (a) engineering stress-engineering strain curves; (b) instantaneous work hardening exponent as a function of true strain; and (c) comparison of mechanical properties between steel A and steel B.

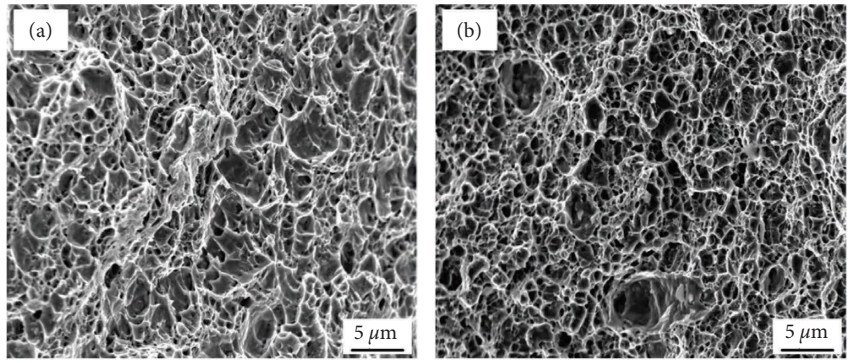


Figure 7: Impact fracture morphologies of experimental steels at −20°C. (a) Steel A. (b) Steel B.

steel B is as high as 18.1 GPa%, which is much higher than the strong plastic product of steel A (13.0 GPa%). As shown in Figure 3, the grain size of A and B steels is calculated by using the intercept method. It is found that the grain size of B steel is 2 times smaller than that of A steel. Therefore, reducing the grain size will enhance the comprehensive mechanical properties of the steel, especially the toughness. It can be found that when the coiling temperature drops to 540°C, the mechanical properties of steel B have met the requirements of the national standard for DP780 dual-phase steel, which is mainly due to the improvement of structure strengthening and precipitation strengthening. The relationship between work hardening index and true strain of experimental steel is shown in Figure 6(b). In the early stage of deformation (true strain <0.075), the work hardening index decreased significantly, and the work hardening index of the two experimental steels was almost the same. Dislocation slip in ferrite at this stage provides the main work hardening, and the interaction of high-density dislocations will lead to a decrease in the length of the active dislocation chain, which ultimately leads to an increase in flow stress [20]. When the deformation continues (true strain <0.032), the work hardening index of steel A gradually decreases, but it is higher than that of steel B. At this stage, the TRIP effect may occur prematurely because of retained austenite in steel A. The work hardening index of B steel gradually increases after the true strain is greater than 0.012. When the true strain is greater than 0.032, its value is higher than that of steel A, indicating that the forming performance of steel B is better than that of steel A. It is reported that the difference of work hardening index of steel A and B is related to TRIP effect austenite and high-density dislocations [21]. The retained austenite in steel B can still have the TRIP effect at relatively large strains, and the fine hard phase structure such as bainite or MA can provide high-density dislocations. Besides, wrong delivery and entanglement also improve the work hardening ability [21, 22]. The work hardening index "$n$" is calculated as follows:

$$n = \frac{d\sigma}{d\varepsilon} \bullet \frac{\varepsilon_T}{\sigma_T}, \quad (1)$$

where $\varepsilon_T$ and $\sigma_T$ are the strain and stress measured, respectively, and $d\varepsilon$ and $d\sigma$ are ture strain and stress, respectively.

When $n = \varepsilon$ during the stretching process, the experimental steel was necked, and the uniform elongation of steel B was 13.5%, which was higher than 5.7% of steel A. The impact energy of steel A and steel B at −20°C are 81.5 J and 93.1 J, respectively. The low-temperature impact fracture morphology of the two experimental steels is shown in Figure 7, showing uniform and small dimples, which are typical ductile fractures. It can be seen from Figure 6(c) that the comprehensive mechanical properties of steel B are better than steel A, and the experimental steel structure type is ferrite/bainite dual-phase steel. Thus, the coiling temperature of 540°C can be as a coiling process to product DP780 grade dual-phase steel.

## 4. Conclusions

Through reasonable composition design, high-strengthhot-rolled ferrite/bainite dual-phase steel can be produced through the TMCP process and the coiling process. When the coiling temperature is 540°C, the yield strength of the experimental steel, the tensile strength, and elongation are 663 MPa, 785 MPa, and 23% respectively, and the strong plastic product is as high as 18.1 GPa%. Its mechanical properties meet the requirements of the DP780 level dual-phase steel national standard. The coiling temperature is too high, the microstructure is relatively coarse and it is not conducive to obtaining uniform and fine VC precipitates, resulting in a decrease in yield strength and tensile strength. The experimental steel with a coiling temperature of 540°C has a uniform elongation of 13.5%, and the work hardening effect is significant at higher strains. The work hardening index is higher than that of the experimental steel with

a coiling temperature of 570°C, and its forming properties are excellent.

## Data Availability

The data used to support the findings of the study are available within the article.

## Conflicts of Interest

The authors declare that they have no conflicts of interest.

## Acknowledgments

This work was supported by the Qinghai Provincial Science and Technology Plan (2022-ZJ-742).

## References

[1] T. Li, L. S. Han, X. B Zheng, B. C. Wang, and Y. Yao, "Influence of factors on edge crack of high strength steel," *Journal of Plasticity Engineering*, vol. 24, no. 4, p. 173, 2017.

[2] G. Yuan, C. N Li, D. D Sun, J. B Kang, and G. D. Wang, "Development status of hot rolled dual-phase steel and development of high strength hot rolled dual-phase steel," *Engineering and Science*, vol. 16, no. 2, p. 39, 2014.

[3] Z. Ding, W. J. Yang, K. F. Huo, and L. O. Shaw, "Thermodynamics and kinetics tuning of $LiBH_4$ for hydrogen storage," *Progress in Chemistry*, vol. 33, no. 9, pp. 1586–1597, 2021.

[4] C. L. Guan and L. H Han, "Development of hot rolling product as the substitution of cold rolling product by boron micro-alloy technology," *Steelmak*, vol. 29, no. 1, p. 28, 2013.

[5] M. Cai, H. Ding, J. Zhang, L. Li, and Z. Tang, "Deformation and fracture characteristics of ferrite/bainite dual-phase steels," *Chinese Journal of Materials Research*, vol. 23, no. 1, p. 83, 2009.

[6] Z. Q. Tian, D. Tang, H. T Jiang, and M. Ceng, "Refinement mechanism of ultrafine-grainvanadium-containing dual phase steel," *Journal of University of Science and Technology Beijing*, vol. 32, no. 1, p. 32, 2010.

[7] A. S. Podder, D. Bhattacharjee, and R. K. Ray, "Effect of martensite on the mechanical behavior of ferrite-bainite dual phase steels," *ISIJ International*, vol. 47, no. 7, pp. 1058–1064, 2007.

[8] A. Kumar, S. Singh, and K. Ray, "Influence of bainite/martensite-content on the tensile properties of low carbon dual-phase steels," *Materials Science and Engineering A*, vol. 474, no. 1-2, pp. 270–282, 2008.

[9] Z. Ding, H. Li, and L. Shaw, "New insights into the solid-state hydrogen storage of nanostructured $LiBH_4$-$MgH_2$ system," *Chemical Engineering Journal*, vol. 385, Article ID 123856, 2020.

[10] M. Jitsukawa and Y. Hosoya, "NKK's state-of-the-art flat-rolled products developed in the last decade," *NKK Technical Review*, vol. 88, p. 46, 2003.

[11] B. Gao, X. Chen, Z. Pan et al., "A high-strength heterogeneous structural dual-phase steel," *Journal of Materials Science*, vol. 54, no. 19, pp. 12898–12910, 2019.

[12] B. Gao, R. Hu, Z. Pan et al., "Strengthening and ductilization of laminate dual-phase steels with high martensite content," *Journal of Materials Science & Technology*, vol. 65, pp. 29–37, 2021.

[13] J. X. Huang, Y. Liu, T. Xu et al., "Dual-phasehetero-structured strategy to improve ductility of a low carbon martensitic steel," *Materials Science and Engineering A*, vol. 834, Article ID 142584, 2022.

[14] Z. Pan, B. Gao, Q. Lai et al., "Microstructure and mechanical properties of a cold-rolledultrafine-graineddual-phase steel," *Materials*, vol. 11, no. 8, p. 1399, 2018.

[15] Z. Q. Tian, D. Tang, H. T Jiang, X. L. Ma, and H. X. Xu, "Research and production status of dual phase steels for automobiles," *Materials for Mechanical Engineering*, vol. 33, no. 4, p. 1, 2009.

[16] Y. J. Li, M. F Liu, H. L. Hu, J. Y. Yang, M. R. Liu, and G. D Wang, "Research on hot-rolling DQ&P process under non-isothermal carbon partition," *Steel Rolling*, vol. 32, no. 2, p. 13, 2015.

[17] S. Morito, H. Yoshida, T. Maki, and X. Huang, "Effect of block size on the strength of lath martensite in low carbon steels," *Materials Science and Engineering A*, vol. 438-440, no. 1, pp. 237–240, 2006.

[18] Z. Ding, S. Li, Y. Zhou et al., "$LiBH_4$ for hydrogen storage-New perspectives," *Nano Materials Science*, vol. 2, no. 2, pp. 109–119, 2020.

[19] J. Zhao, T. Lee, J. H. Lee, Z. Jiang, and C. S. Lee, "Effects of tungsten addition on the microstructure and mechanical properties of microalloyed forging steels," *Metallurgical and Materials Transactions A*, vol. 44, no. 8, pp. 3511–3523, 2013.

[20] J. Galan, L. Samek, P. Verleysen, K. Verbeken, and Y. Houbaert, "Advanced high strength steels for automotive industry," *Revista de Metalurgia*, vol. 48, no. 2, pp. 118–131, 2012.

[21] X. Tan, Y. B. Xu, X. Yang, and D. Wu, "Microstructure–properties relationship in a one-step quenched and partitioned steel," *Materials Science and Engineering A*, vol. 589, no. 589, pp. 101–111, 2014.

[22] F. Peng, Y. B. Xu, D. Han, X. Gu, J. Li, and X. Wang, "Influence of pre-tempering treatment on microstructure and mechanical properties in quenching and partitioning steels with ferrite-martensite start structure," *Materials Science and Engineering A*, vol. 756, no. 756, pp. 248–257, 2019.